Modeling of Initially Subcooled Flashing Vortex Flow in the Nozzle for Possible Applications in the Control of Ejector Cooling Cycles

Presenter: Jingwei ZHU

Stefan ELBEL

University of Illinois at Urbana-Champaign
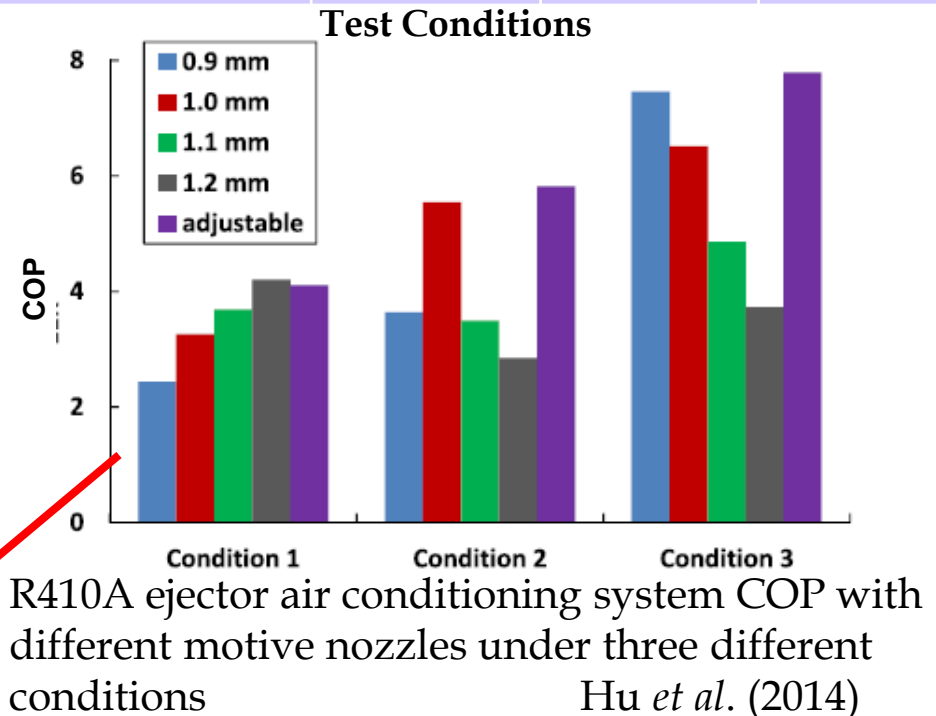Department of Mechanical Science and Engineering

July 11 -14, 2016

Challenges with Ejector Cooling Cycle

- **Different working conditions/capacities favor different ejector geometry** Elbel and Hrnjak (2008); Elbel (2011);

- **Slightly different geometry might result in significant difference in system COP under the same conditions** Sumeru *et al.* (2012); Sarkar (2012);

- **Ejector motive nozzle throat diameter (nozzle restrictiveness) is one of the key points that can significantly affect COP**
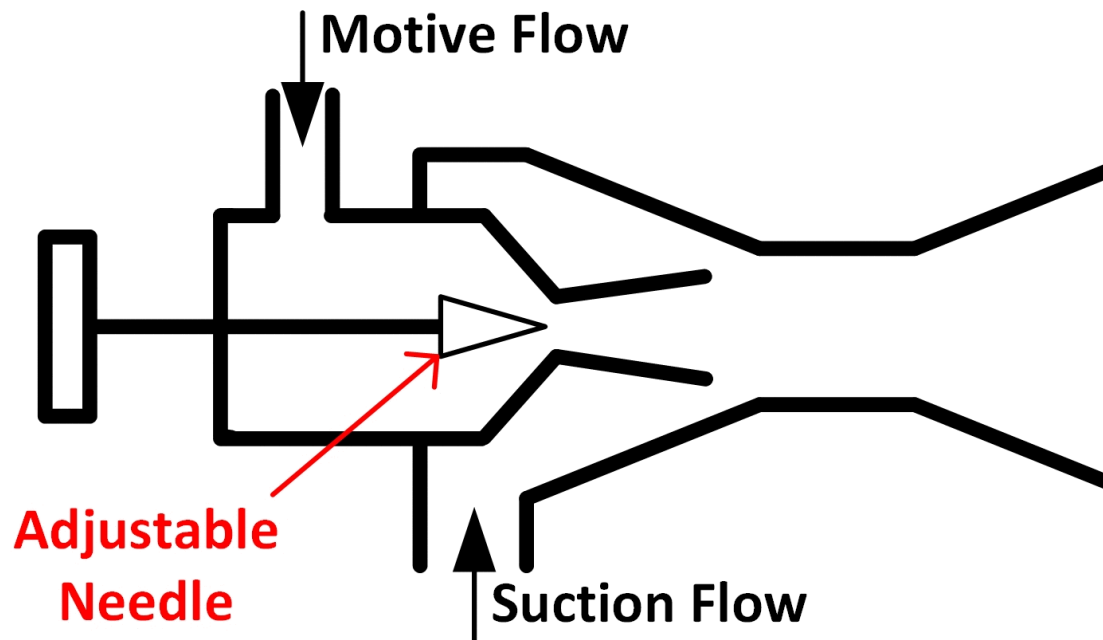
  COP changed by more than 40 %

	Condition 1	Condition 2	Condition 3
T_{indoor} (dry/wet bulb), ^{o}C	26.7/19.4	26.7/19.4	26.8/19.5
$T_{outdoor}$ (dry/wet bulb), ^{o}C	35.0/19.5	30.6/16.8	27.8/14.9
p_{cond}, MPa	2.4	2.0	1.9

Test Conditions

R410A ejector air conditioning system COP with different motive nozzles under three different conditions   Hu *et al.* (2014)
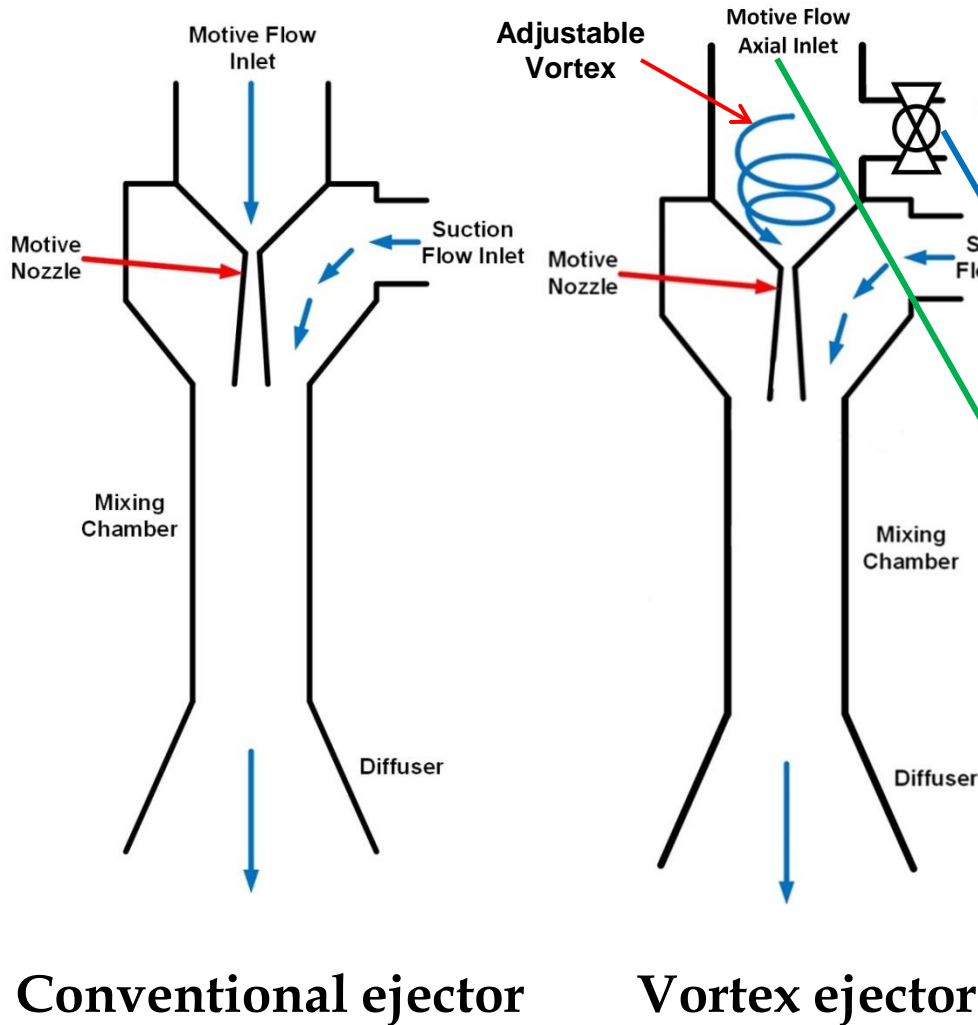
Previous Approaches

- Ejectors in parallel
- Ejector with adjustable needle

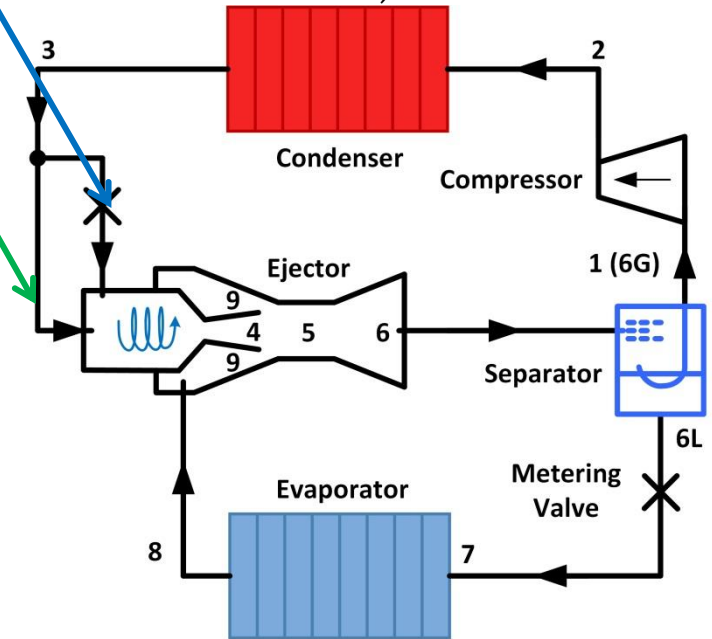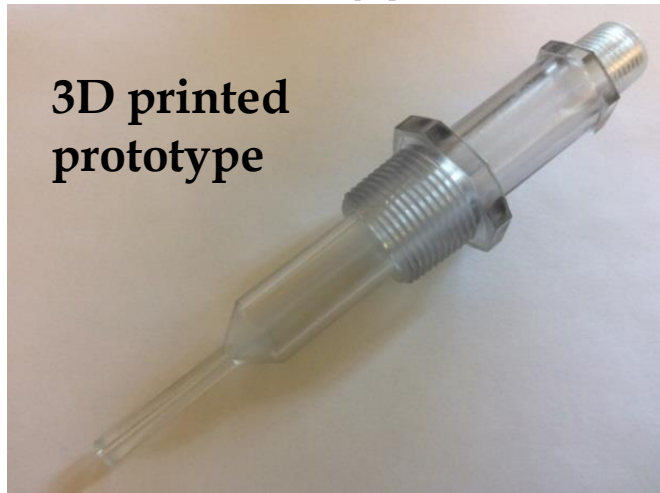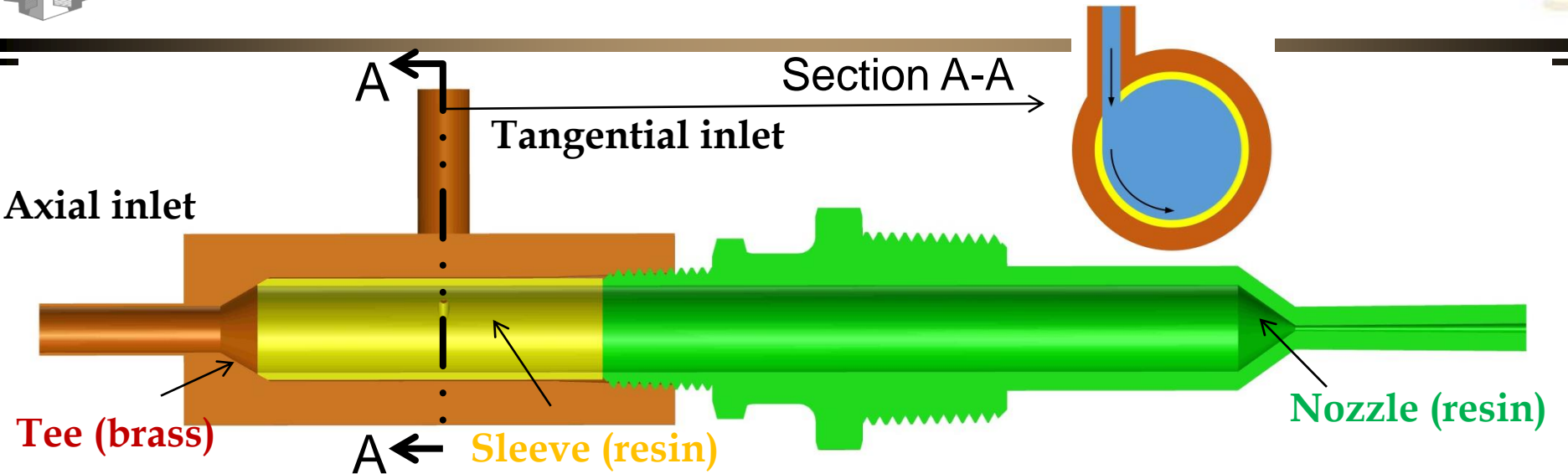# New Solution: Vortex Ejector

Utilizing an adjustable vortex at the motive inlet to control the flow expanded in the motive nozzle (no change in geometry; same effect as changing nozzle throat diameter)

Conventional ejector

Vortex ejector

Vortex ejector cooling cycle

Vortex Nozzle

Axial inlet

A ← (Section cut line)

Tangential inlet

Section A-A →

Tee (brass)

A ←

Sleeve (resin)

Nozzle (resin)

3D printed prototype

Convergent-divergent nozzle (resin)

| Nozzle inlet diameter (mm)	15.0
Nozzle throat diameter (mm)	1.03
Nozzle outlet diameter (mm)	1.7
Nozzle convergent part length (mm)	9.9
Nozzle divergent part length (mm)	40.0
Tangential inlet inner diameter (mm)	2.0
Vortex decay distance (mm)	138.0

Vortex nozzle geometry

Axial velocity profile

Tangential velocity profile

Inlet

Nozzle convergent part

Inlet

Outlet

Outlet

$$\Delta p \sim \frac{1}{2}\rho\left(V_{out}^2 - V_{in}^2\right)$$

$$V_{out}^2 = V_{axial,out}^2 + V_{tangential,out}^2$$

$$\dot{m} \sim \rho V_{axial,out} A_{out}$$
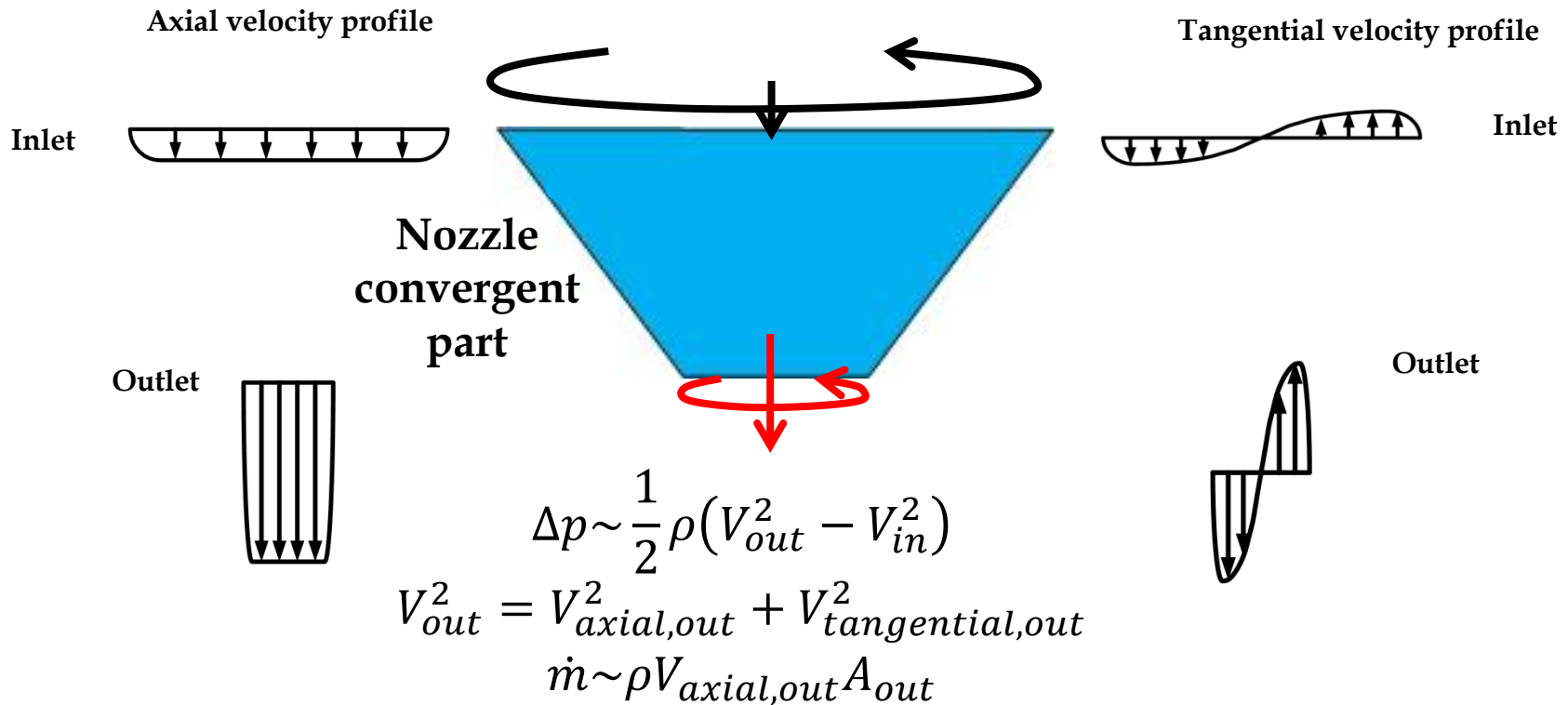
Works for both single-phase and two-phase

Choked Mass Flow Rate with Different Inlet Vortex Strengths at Constant Inlet Pressure
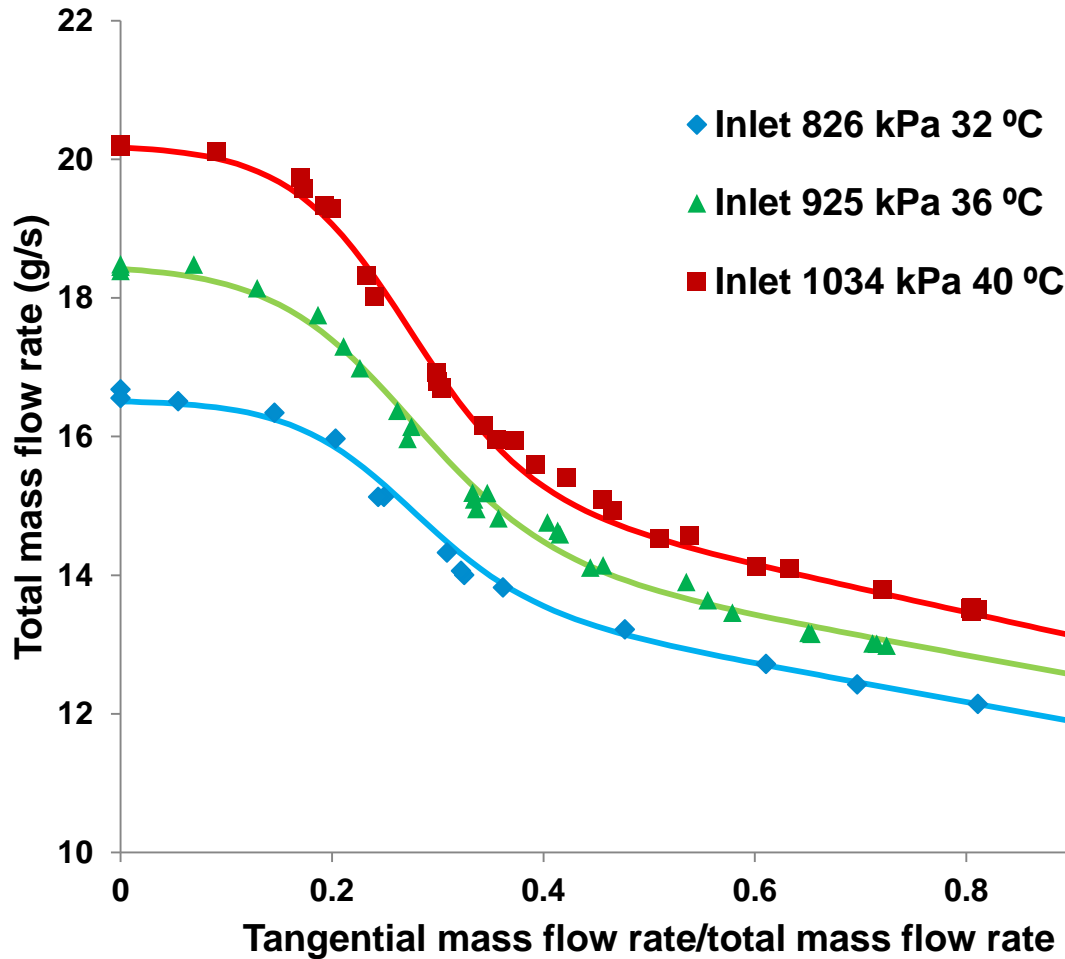
Refrigerant: R134a
Inlet subcooling = 0.5 °C

Mass flow rate can be reduced by 35 % with vortex under the same inlet and outlet conditions (large control range).

Nozzle restrictiveness on the flow is changed by vortex; the stronger the vortex is, the larger the restrictiveness is.
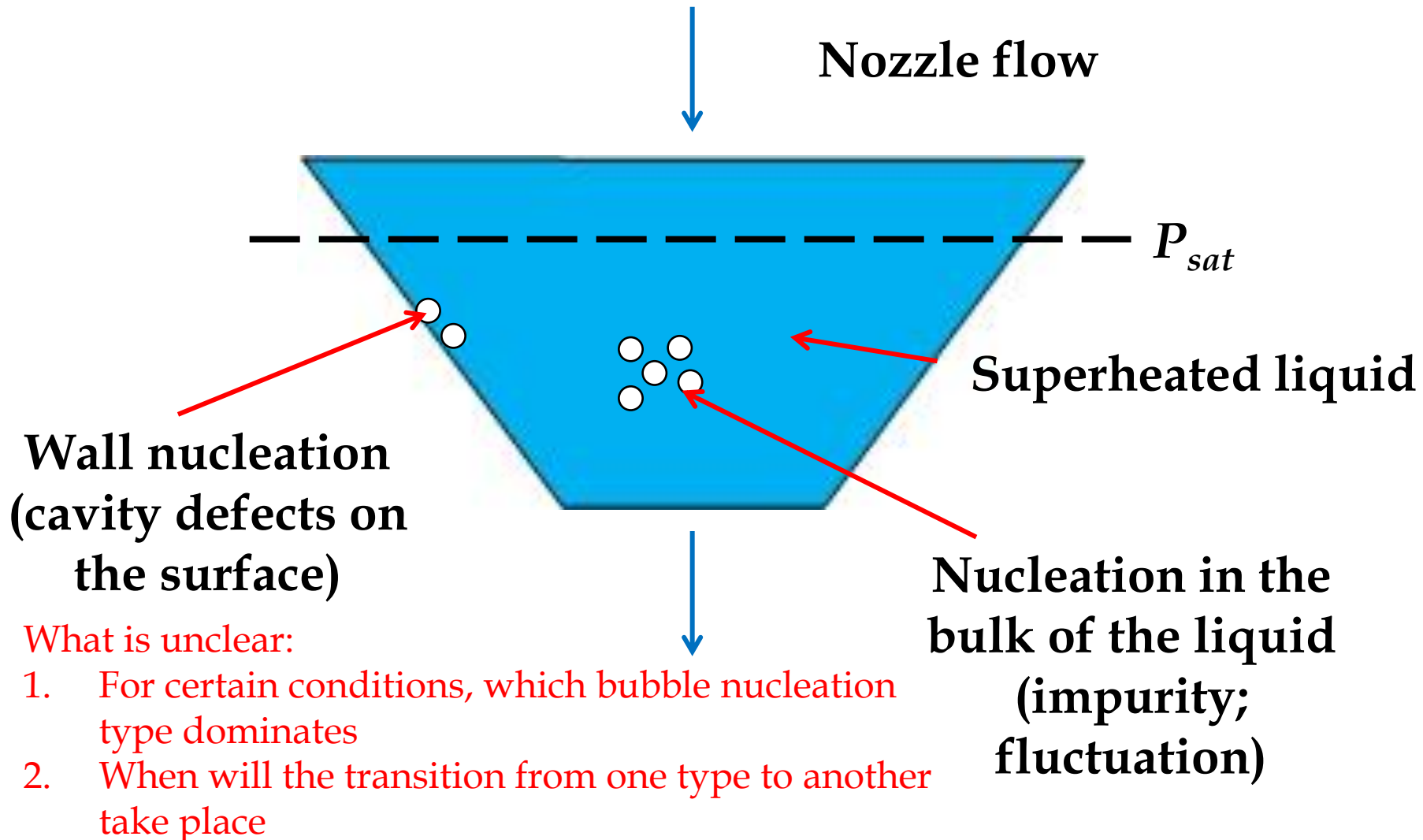
- Bubble nucleation
- Two modeling approaches
- Governing equations
- Solution procedure
- Comparison of the modeling results with the experimental results

Note: In this paper, only the convergent part of the nozzle is considered. It is assumed that the choked mass flow rate through the nozzle is only determined by the convergent part.
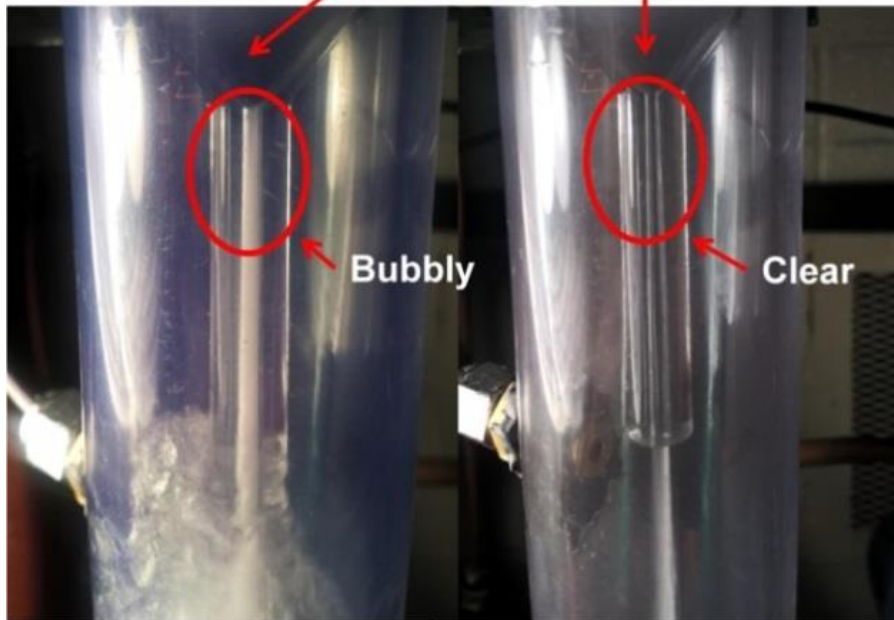
Bubble Nucleation

Nozzle flow

P_{sat}

Superheated liquid

Wall nucleation (cavity defects on the surface)

Nucleation in the bulk of the liquid (impurity; fluctuation)

What is unclear:
1. For certain conditions, which bubble nucleation type dominates
2. When will the transition from one type to another take place

Clear flow in the convergent part of the nozzle

Bubbly

Clear

(a)

(b)

Choked flow (very low outlet pressure): becomes bubbly immediately after the throat

Outlet pressure close to inlet pressure: flow is still clear after the throat

Zhu, Elbel (2016)

Superheated liquid

Two-phase mixture

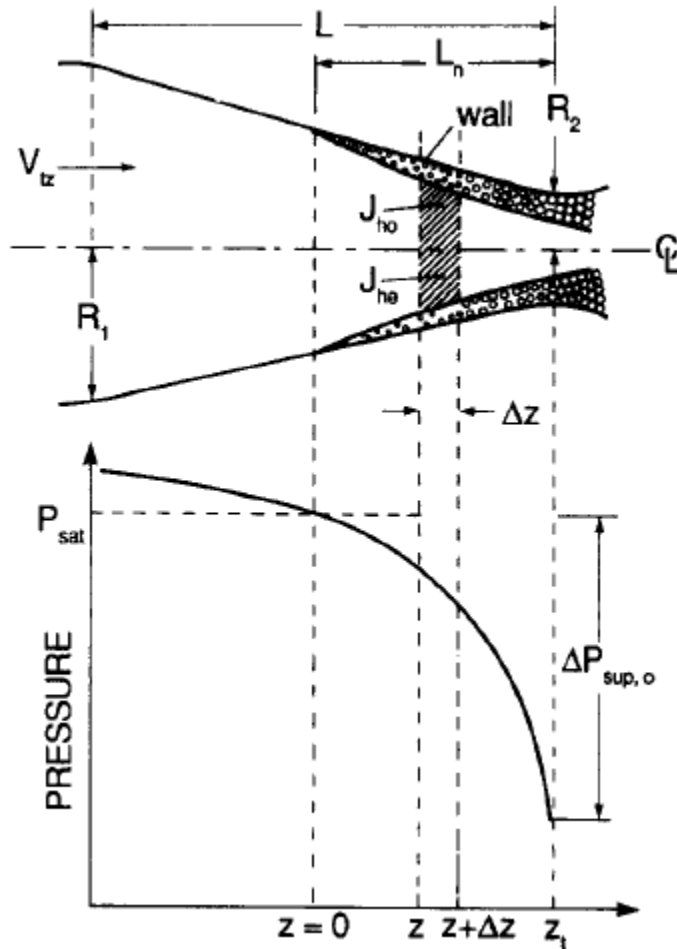**Image of an evaporation wave in progress**

Benoit Stutz, José Roberto Simões-Moreira (2013)

Assumption:
- **There is an evaporation wave at the nozzle throat.**
- **The bubble generation in the upstream of the evaporation wave is neglected.**
- **The metastable pressure in the upstream of the evaporation wave keeps constant for the same nozzle inlet pressure and subcooling.**

Assumption:
Bubble nucleation during the depressurization in the nozzle all occurs at the nozzle wall.

Shin and Jones (1993)

Governing Equations

The continuity equation for each phase is

$$\frac{\partial \rho_k}{\partial t} + \nabla \cdot (\rho_k v_k) = 0 \qquad (1)$$

The momentum equation for each phase is

$$\frac{\partial \rho_k v_k}{\partial t} + \nabla \cdot (\rho_k v_k v_k) = -\nabla p_k + \nabla \cdot \varepsilon_k \qquad (2)$$

where ε_k is the viscous stress.

The balance of energy can be written as

$$\frac{\partial \rho_k \left(u_k + \frac{v_k^2}{2}\right)}{\partial t} + \nabla \cdot \left[\rho_k \left(u_k + \frac{v_k^2}{2}\right) v_k\right] = -\nabla \cdot q_k + \nabla \cdot (\sigma_k \cdot v_k) \quad (3)$$

where q_k and σ_k represent the heat flux and the surface stress tensor, respectively.

The interfacial mass balance between the liquid and vapor phases is

$$\sum_{k=1}^{2} \dot{m}_k = 0 \qquad (4)$$

Bubble Departure (In Approach 2 Considering Only Nozzle Wall Nucleation)

Bubble nucleation and departure are assumed to take place at where the liquid superheat is larger than zero.

The departure radius of a bubble is given by (Shin and Jones, 1993)

$$R_{depart} = \sqrt{\frac{\mu_{liquid}}{\tau_{wall}} \sqrt{\frac{4\sigma R_c}{C_D \rho_{liquid}}}} \tag{5}$$

where the drag coefficient C_D is assumed to be 0.5, R_c is the minimum cavity size and is approximated as

$$R_c \approx \frac{2\sigma T_{sat}}{\rho_{vapor} h_{fg}(T_{liquid} - T_{sat})} \tag{6}$$

The frequency of bubble departure per unit area is assumed to be

$C_{depart}(T_{liquid} - T_{sat})^3$ (Shin and Jones, 1993), where C_{depart} is a constant.

Governing Equations

- **Single Bubble Motion (In Approach 2 Considering Only Nozzle Wall Nucleation)**
- **Bubble Growth (In Approach 2 Considering Only Nozzle Wall Nucleation)**
- **Boundary Conditions**

The flow at the nozzle inlet is subcooled liquid. There is no bubble mass flow rate entering the nozzle through the inlet.

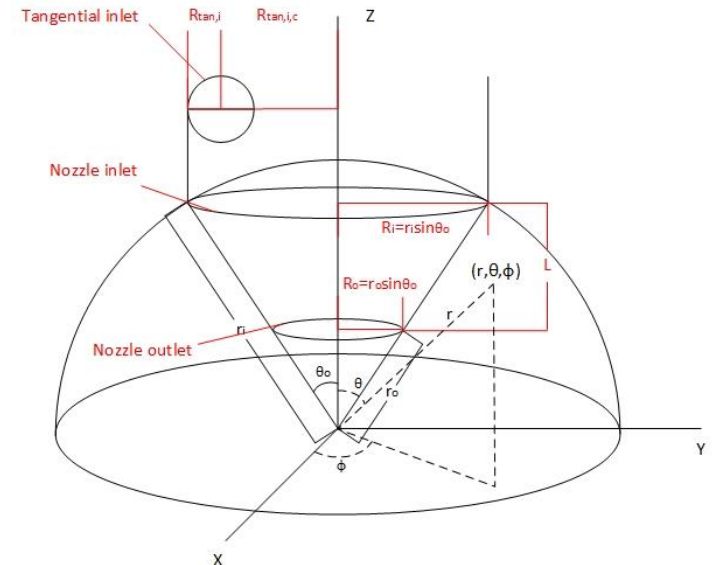$$v_r(r_i, \theta) = -\frac{\dot{m}_{total}}{2\pi r_i^2 \rho_{liquid}(1 - \cos \theta_o)} \quad (7)$$

$$v_\theta(r, \theta_o) = 0 \quad (8)$$

$$v_\phi(r_i, \theta) = v_\phi(r_i, \theta_o)\frac{\sin \theta}{\sin \theta_o} \quad (9)$$

$$p(r_i, \theta_o) = p_i \quad (10)$$

$$p(r_o, 0) = p_o \quad (11)$$

$$T(r_i, \theta) = T_i \quad (12)$$

Solution Procedures

Liquid Flow Field Assumption

It is assumed that the vapor mass flow rate in the nozzle compared with that of liquid is negligible. Therefore, $\dot{m}_{total} \approx \dot{m}_{liquid}$.

The liquid velocity field in the whole computational domain of the convergent nozzle is assumed to be

$$v_r(r, \theta) = v_r(r) \tag{13}$$

$$v_\theta(r, \theta) = 0 \tag{14}$$

$$v_\phi(r, \theta) = v_\phi(r, \theta_o) \frac{\sin \theta}{\sin \theta_o} \tag{15}$$

Solution Procedures

Wall Shear Stress Modeling

The wall shear stress is modeled as:

$$\tau_{wall}(r) = \frac{1}{8}\lambda\rho_{liquid}[v_r^2(r,\theta_o) + v_\phi^2(r,\theta_o)] \qquad (16)$$

where λ is the Darcy–Weisbach friction factor which is modeled as a function of surface roughness ϵ and Reynolds number Re:

$$\frac{1}{\sqrt{\lambda}} = -2\,log_{10}(\frac{\epsilon}{3.7D} + \frac{5.74}{Re^{0.9}}) \quad \text{(Swamee–Jain equation)} \qquad (17)$$

$$Re = \rho_{liquid}\sqrt{v_r^2(r,\theta_o) + v_\phi^2(r,\theta_o)}D_N/\mu_{liquid} \qquad (18)$$

where the nozzle diameter $D_N = 2R_N = 2rsin(\theta_o)$.

$$\tau_\phi(r) = -\frac{v_\phi(r,\theta_o)}{\sqrt{v_r^2(r,\theta_o) + v_\phi^2(r,\theta_o)}}\tau_{wall}(r) \qquad (19)$$

$$\tau_r(r) = -\frac{v_r(r,\theta_o)}{\sqrt{v_r^2(r,\theta_o) + v_\phi^2(r,\theta_o)}}\tau_{wall}(r) \qquad (20)$$
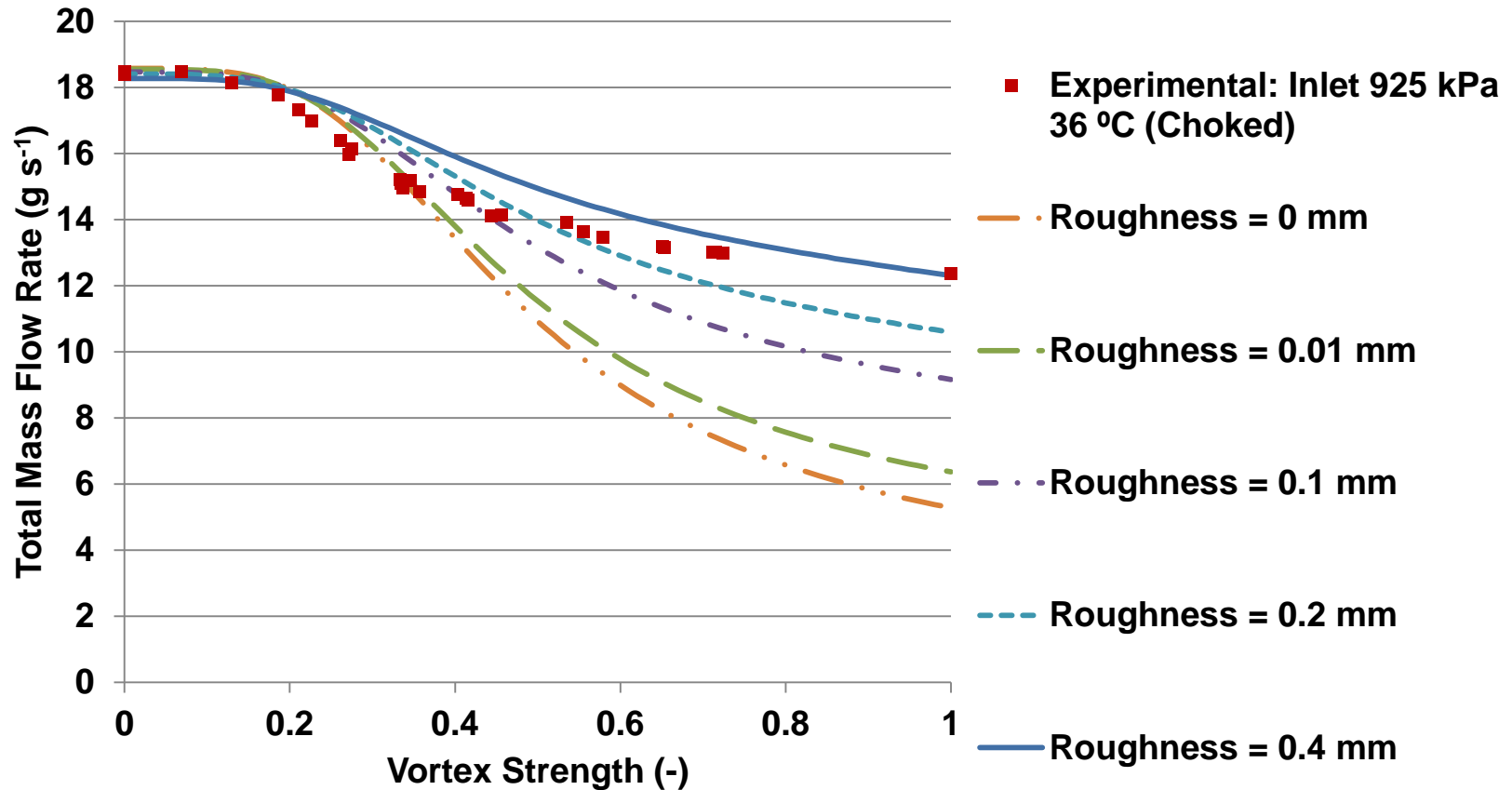
Solution Procedures

Numerical Methods

- The governing equations have been discretized based on the finite volume method.
- The bubble motion and growth is approximated by Euler method. The contributions of vapor in the mass and momentum equations are regarded as negligible.
- The momentum equations are discretized by using first order upwind differencing. The shear stress from the velocity gradient in the radial direction is not considered.
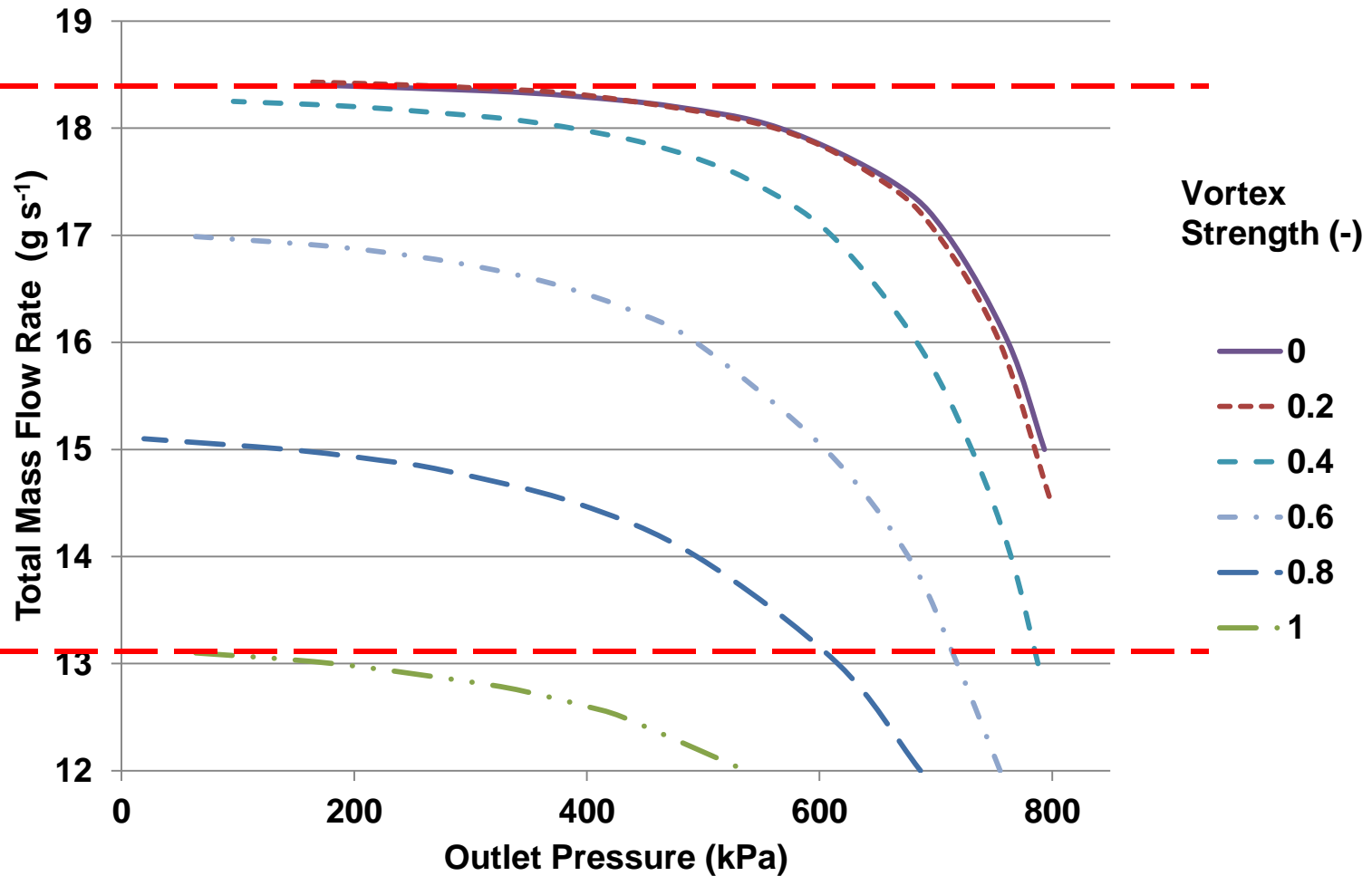
Modeling Results (Approach 2)

Experimental Results
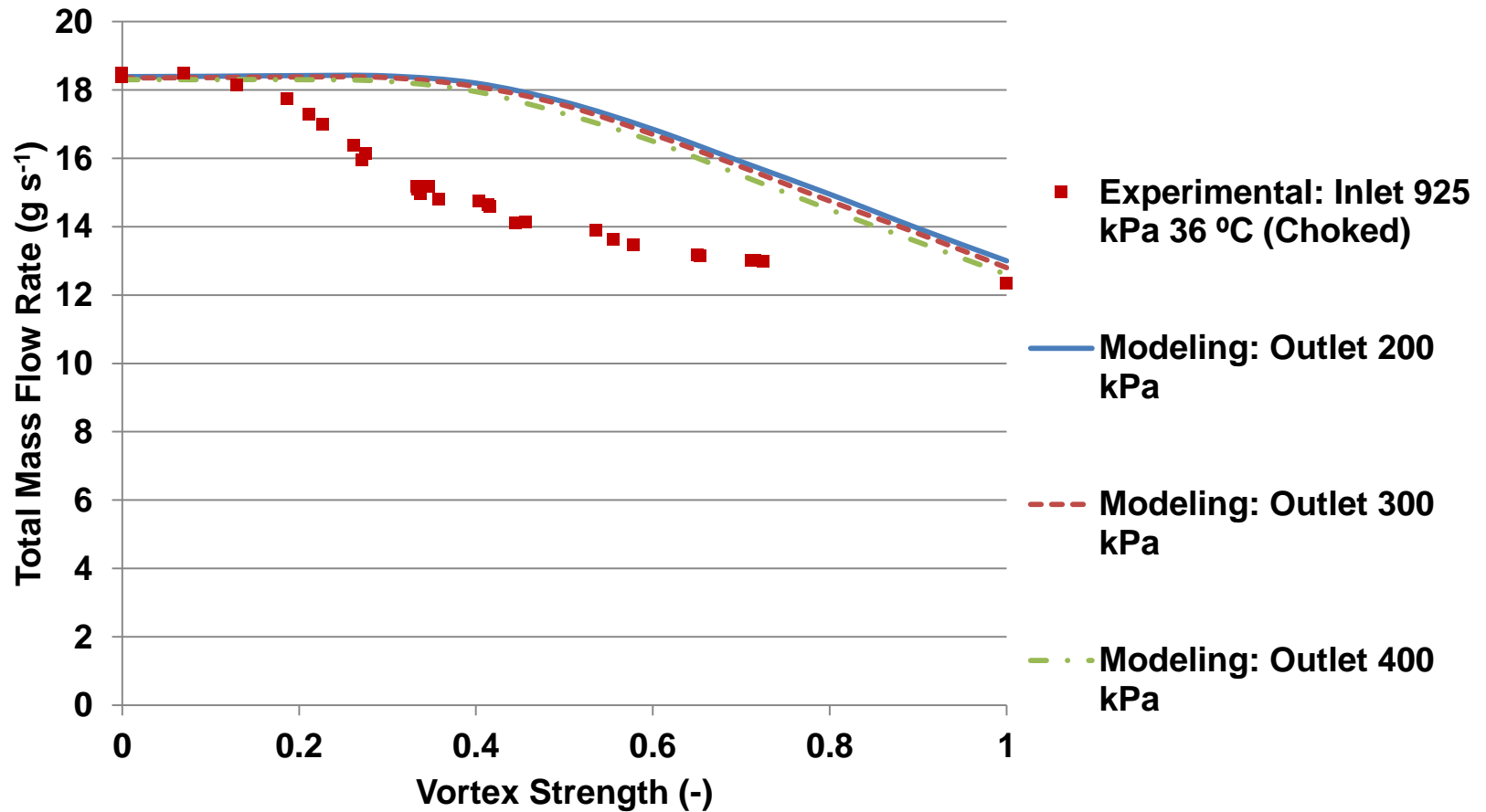
Summary and Conclusions

- The bubble nucleation may not all occur at the nozzle wall at high degree of metastability. Nucleation in the bulk of the liquid might be dominant and should possibly be taken into consideration in the modeling.
- The change in total mass flow rate is smaller for the same inlet vortex strength with larger surface roughness.
- The discrepancies between the modeling and experimental results might be due to
  - oversimplification of the flow velocity profile and inappropriate turbulent wall shear stress model
  - influence of vortex strength and depressurization rate on the maximum achievable degree of metastability
  - decay of vortex strength as the vortex flow travels from the vortex nozzle tangential inlet to the starting point of the convergent part of the nozzle

Thank you for your attention!
Any questions?

- Presenter: Jingwei Zhu

- Email: jzhu50@illinois.edu

- Acknowledgments: The authors would like to thank the member companies of the Air Conditioning and Refrigeration Center at the University of Illinois at Urbana-Champaign for their generous support.